CONICET

Joint ICTP-IAEA School on
Novel Experimental Methodologies for Synchrotron Radiation Applications in Nano-science and Environmental Monitoring
17 November - 28 November 2014

Grazing-Incidence X-Ray Resonant Raman Scattering (GI-RRS)

Héctor Jorge Sánchez

Facultad de Matemática Astronomía y Física

Universidad Nacional de Córdoba, Córdoba, Argentina

CONICET

Argentina

Basic Photon Interactions

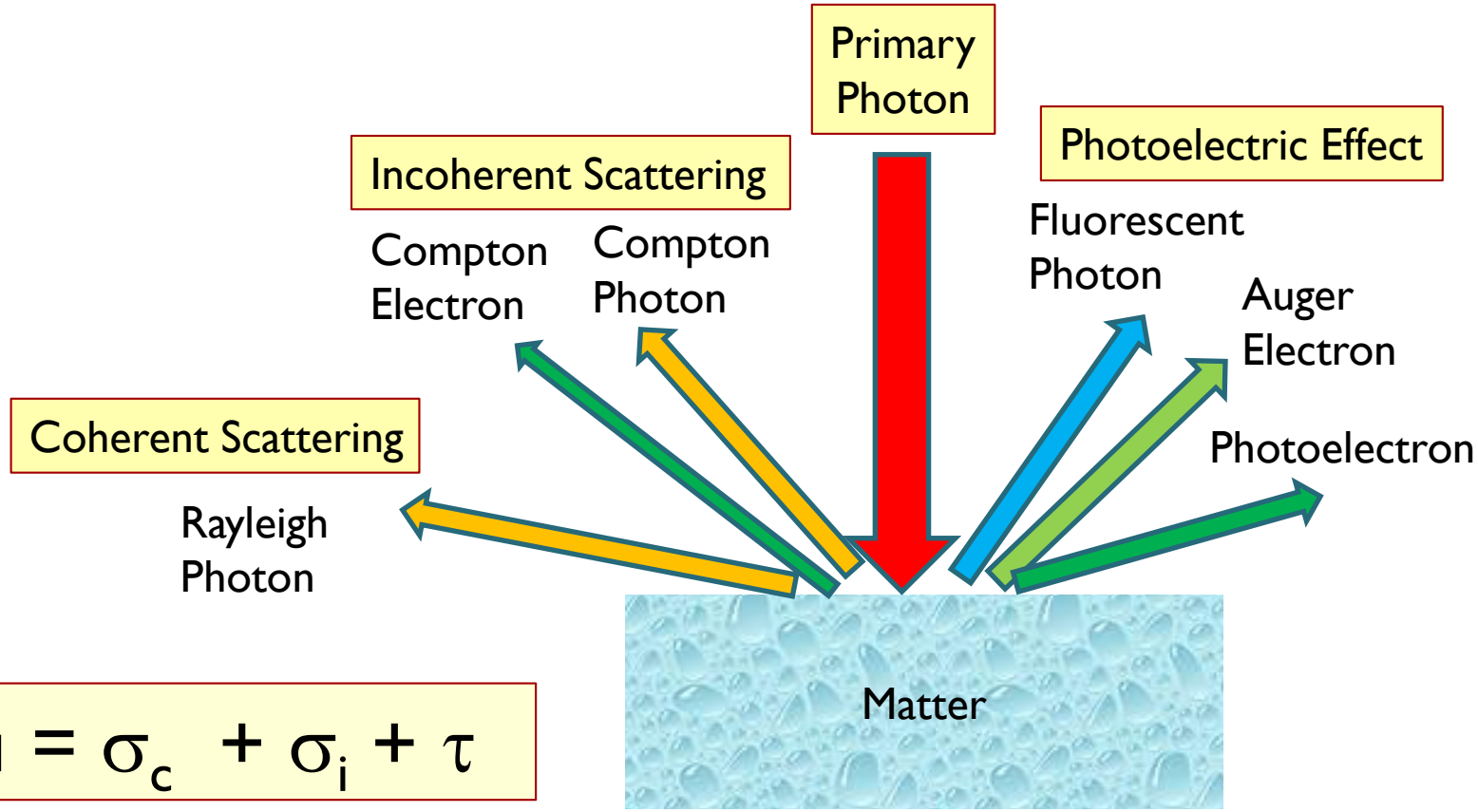

$$\mu = \sigma_c + \sigma_i + \tau$$

Basic Photon Interactions

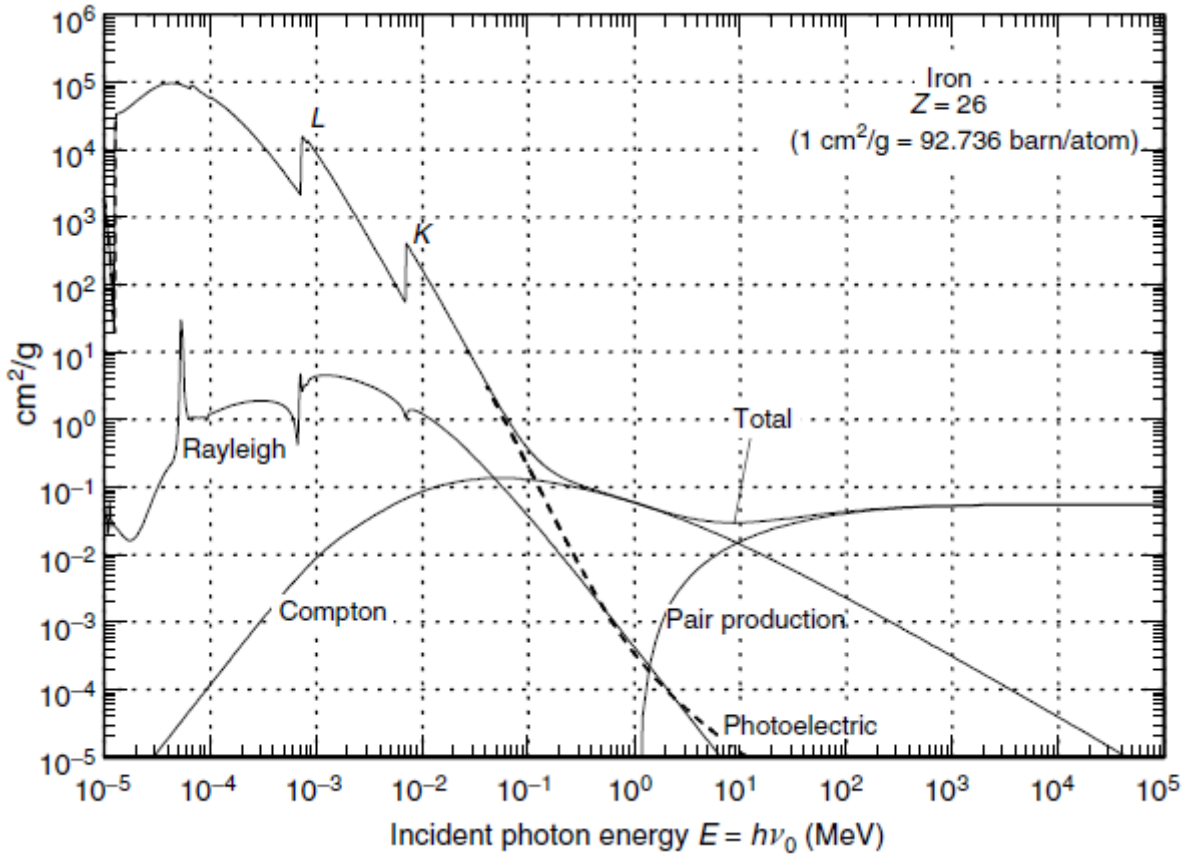

Theoretical Formulation

J. Sherman, *Spectrochim. Acta* **7**, 283 (1955).
T. Shiraiwa and N. Fujino, *Jpn. J. Appl. Phys.* **5**, 886 (1966).

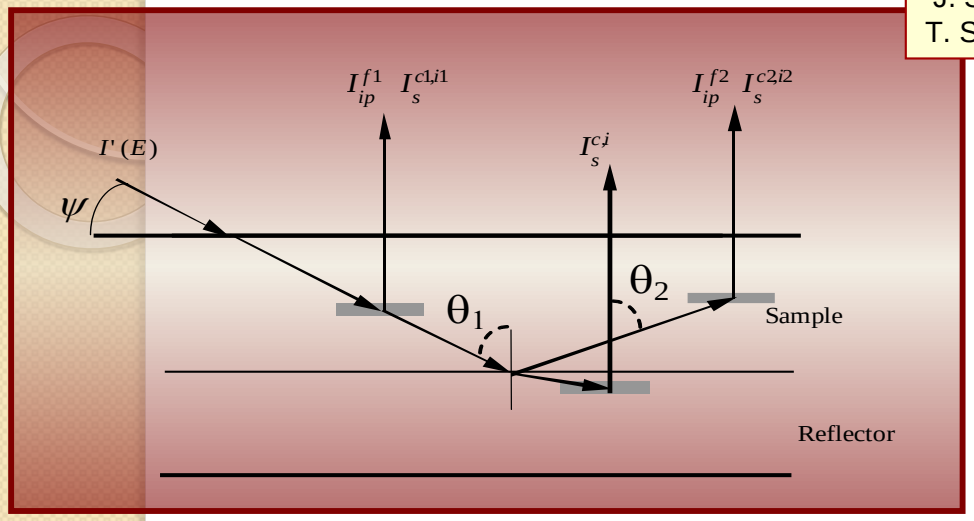

$$Q_k^f(E) = C_k\ \omega_k\ f_k\ J_k\ \tau_k\ (E)$$

$$Q_k^{c,i}(E) = \sum_{k=1}^{N} C_k\ \sigma_k^{c,i}(E)$$

$$ {}^1I_i^x = \int_0^{E_{max}} \int_0^{E_{max}} \frac{\Delta}{4\pi} \frac{I_0(\tilde{E}) Q_i^x(\tilde{E}, E')}{\mu_s(\tilde{E}) - \mu_s(E')G} d\tilde{E} \frac{e^{-\frac{(E-E')^2}{2\delta^2}}}{\sqrt{2\pi}\delta} dE' $$

$$ {}^2I_i^{x,y} = \int_0^{E_{max}} \sum_{k=1}^{N} \int_0^{E_{max}} \frac{\Delta}{8\pi} \frac{I_0(\tilde{E}) Q_k^x(\tilde{E}, E'') Q_i^y(E'', E')}{\mu_s(\tilde{E}) - \mu_s(E')G} \left\{ \frac{\cos\theta_1}{\mu_s(E'')} \ln\left[1 + \frac{\mu_s(\tilde{E})}{\mu_s(E'')\cos\theta_1}\right] + \frac{\cos\theta_2}{\mu_s(E')} \ln\left[1 + \frac{\mu_s(E')}{\mu_s(E'')\cos\theta_2}\right] \right\} d\tilde{E} \frac{e^{-\frac{(E-E')^2}{2\delta^2}}}{\sqrt{2\pi}\delta} dE' $$

Low Probability Processes

- 1st and 2nd Order Photoexcitation (Raman Scattering)
- Nuclear Thomson Scattering
- Nonelastic nuclear scattering (Giant Dipole Resonance, Photodisintegration, Photopion Production, etc.)
- Delbrück scattering
- NEET (Nucleus excitation)
- Multiple Ionization (one photon – two vacancies)
- Multiple Decay (one vacancy – two photons)
- XRF Lines Anisotropy (L – lines)
- Forbidden Transitions (Kb satellite lines)
- Etc. Etc. Etc.

X-Ray Resonant Raman Scattering

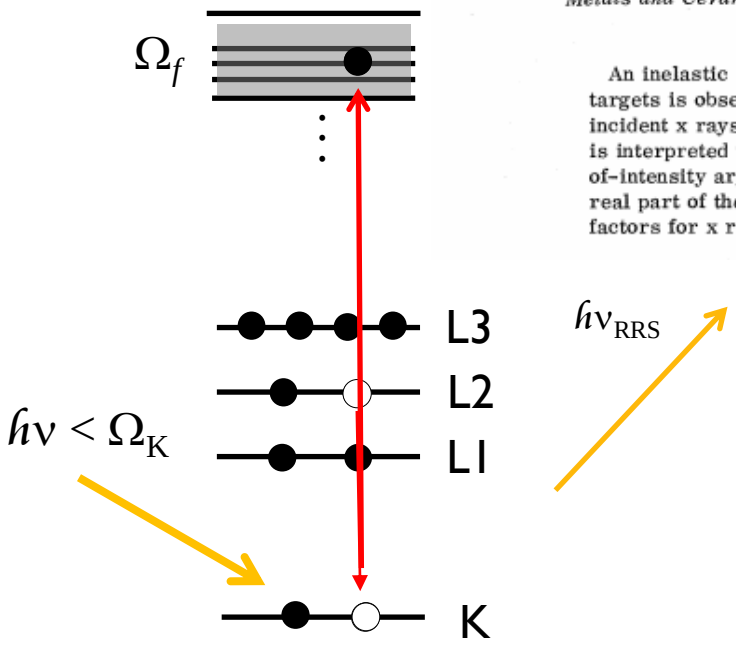

VOLUME 33, NUMBER 5 PHYSICAL REVIEW LETTERS 29 JULY 1974

Inelastic Resonance Emission of X Rays: Anomalous Scattering Associated with Anomalous Dispersion*

Cullie J. Sparks, Jr.
Metals and Ceramics Division, Oak Ridge National Laboratory, Oak Ridge, Tennessee 37830
(Received 13 May 1974)

An inelastic resonance scattering of monochromatic Cu $K\alpha$ x rays incident on various targets is observed when an absorption edge of the target is just above the energy of the incident x rays. This frequency-dependent and angular-independent inelastic scattering is interpreted with the x-ray scattering theory of anomalous dispersion. Conservation-of-intensity arguments allow a comparison of the observed inelastic intensity with the real part of the anomalous dispersion corrections to the coherent atomic scattering factors for x rays.

$$h\nu_{RRS} = h\nu - \Omega_{L2} - \Omega_f - k$$

X-Ray Resonant Raman Scattering

Kramers- Heisenberg ´s Equations
(Time Depending Perturbation Theory)

$$\frac{d\sigma(E_0,E_S)}{dE_S}=\left(\frac{E_S}{E_0}\right)\left(\frac{e^2}{mc^2}\right)^2 c\int\frac{\left(1-n_{\vec{k}}\right)\left|M_{fi}\right|^2\delta\left(E_0-E_s-(u_{\vec{k}}+\Omega_L)\right)d^3k}{8\pi^3}$$

$$M_{fi}=\frac{\langle P|\vec{p}\cdot\vec{u}_2|S\rangle\langle k|\vec{p}\cdot\vec{u}_1|S\rangle}{m(E_0-u_k-\Omega_k+i\Gamma_K)}$$

$$\frac{d\sigma(E_0,E_S)}{dE_S}=G(E_0,E_S)\frac{E_S}{\left(\Omega_K-\Omega_L-E_S\right)^2+\Gamma_K^2}$$

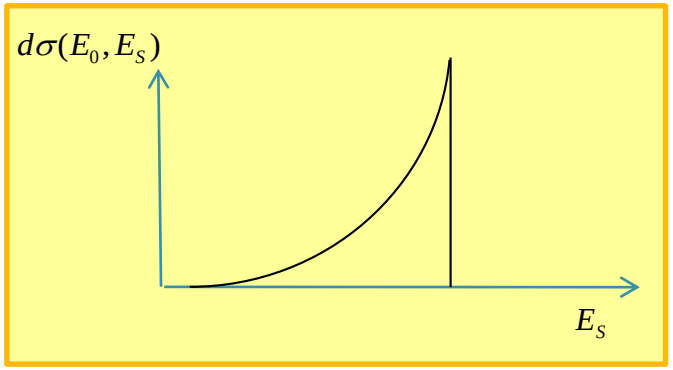

$$\sigma(E_0,E_1)=\Phi\int_0^{E_0-\Omega_L-e_f}\frac{E}{\left(\Omega_K-\Omega_L-E\right)^2}\,\mathrm{e}^{-\frac{(E_1-E)^2}{2\delta^2}}\,dE$$

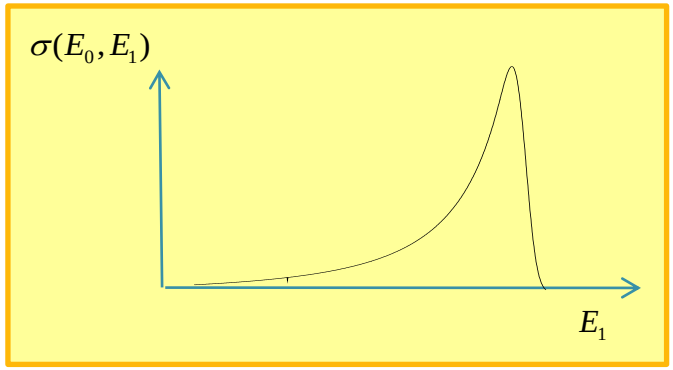

Experimental RRS

- X-Ray Tube (difficult to observe)
- Secondary Target (Simplest way)
- Synchrotron Radiation (Monochromatic Beam)

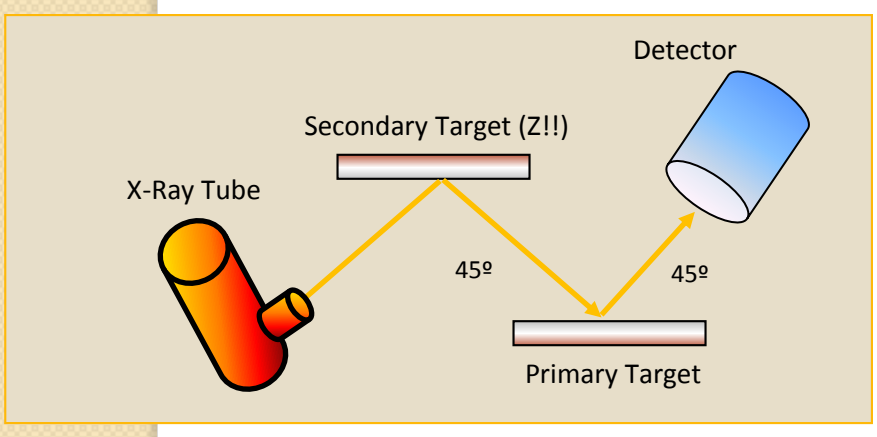

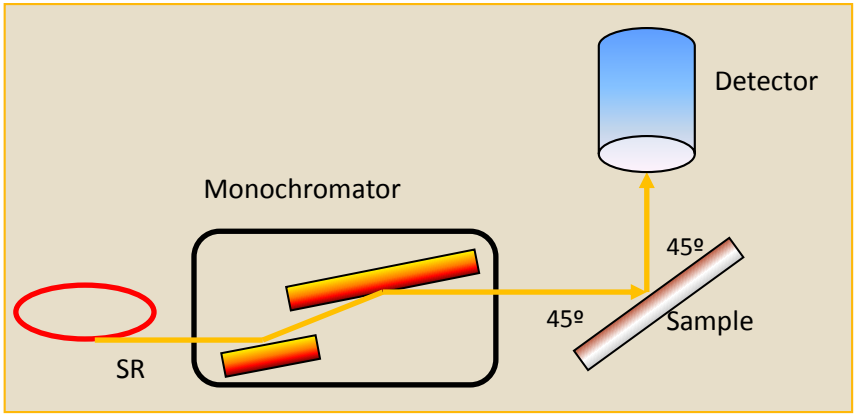

Experimental RRS

XRF Beamline (LNLS)

- Storage ring operating at 3.7 GeV and nominal current of 100 mA.
- Silicon (111) channel-cut double-crystal monochromator. The energy resolution is 3×10^{-4} between 7 and 10 keV.
- A motorized computer-controlled set of vertical and horizontal slits to limit the beam size, before and after the monochromator.
- A ionization chamber to measure the primary beam intensity.
- A Si(Li) solid state detector, with a resolution of 165 eV at 5.9 keV.
- The samples were mounted in a vacuum chamber with a sample holder at 10^{-2} Torr in a standard geometrical configuration of 45◦ of incident and take-off angles.

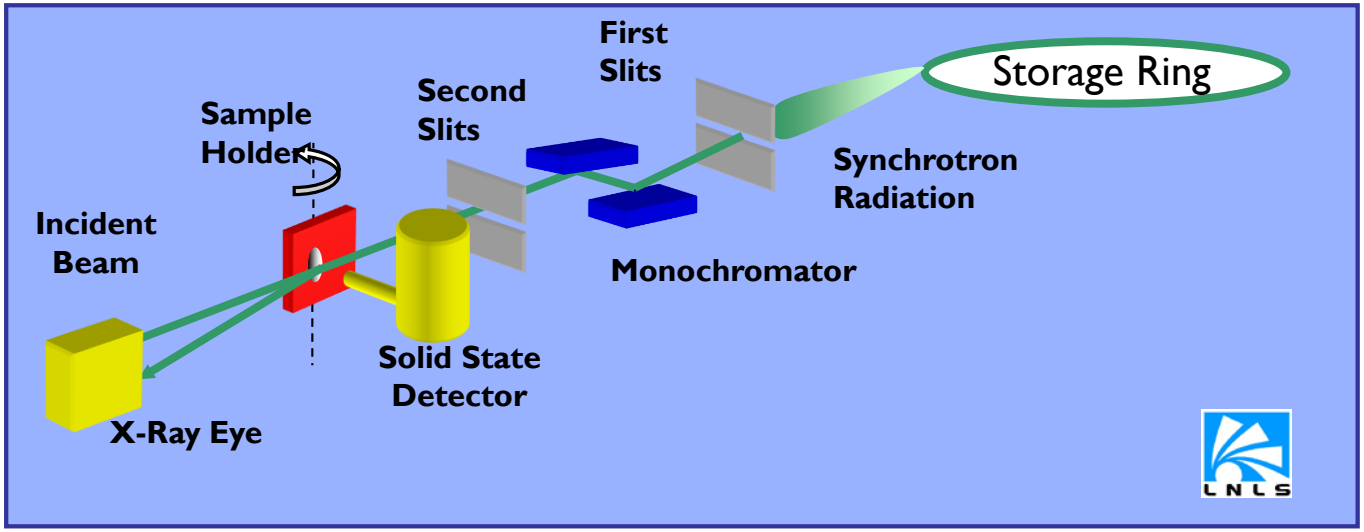

Experimental RRS

LNLS,
D09B Beamline
Channel Cut
monochromator.
Si(Li) Detector

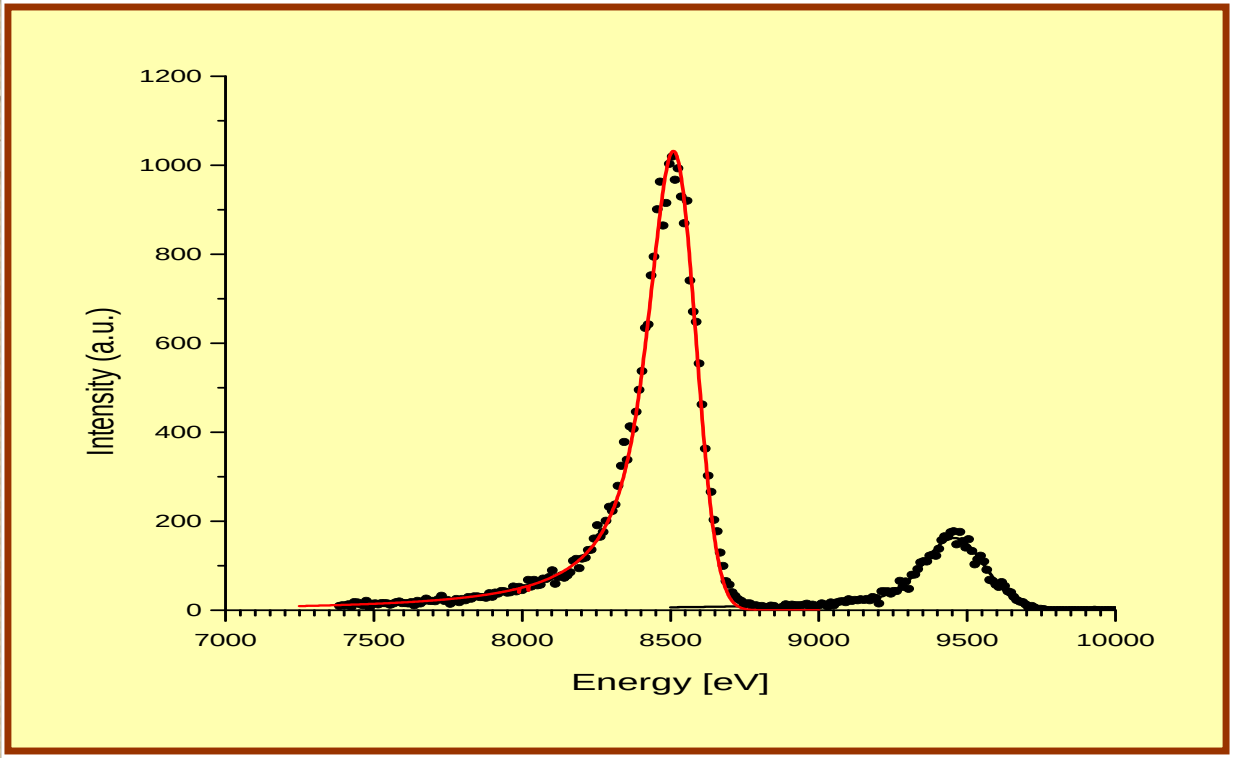

KL-RRS spectrum of Zn obtained with incident energy of 9594 eV. Solid lines represent the data fitting of each peak.

Sánchez, H.J. et al. *J Phys B:At Mol Opt Pys* 2006; **39:** 1-11*h*

RRS Cross Sections

$$\sigma(E_0) = \frac{I_0^F \; I_R \; \tau(E_0)(1-1/R)\, G_F}{I_0^R \; I_F \; G_S}\, \varpi_K$$

$$G_F = \frac{1-\mathrm{e}^{-\frac{2\left(\mu(E_0)+\mu(E_F)\right)d\rho}{\sqrt{2}}}}{\mu(E_0)+\mu(E_F)}$$

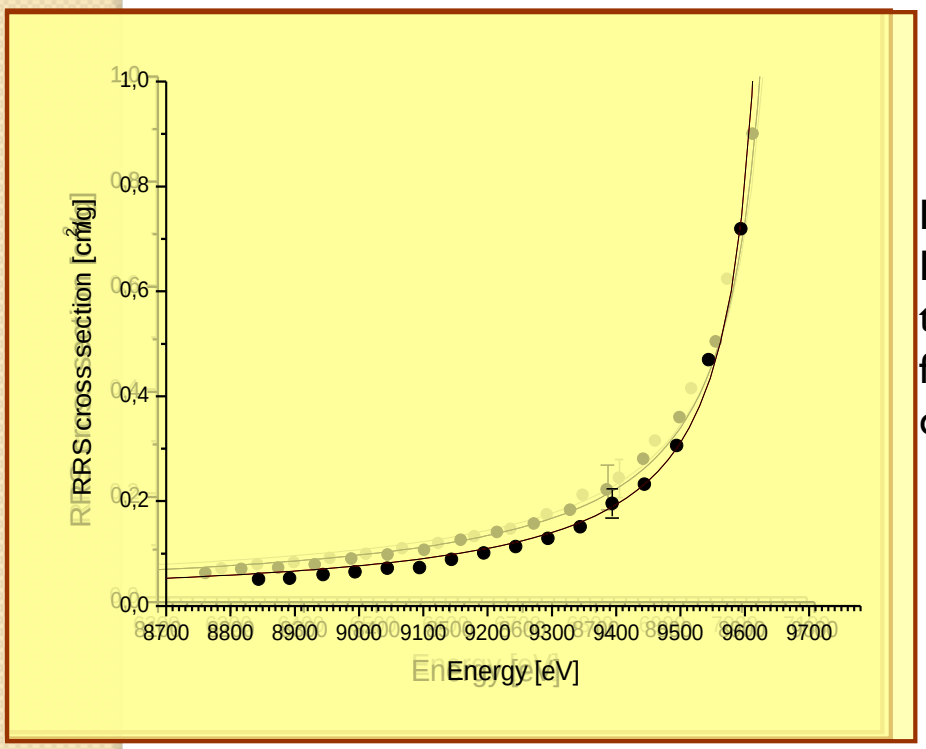

Measured KL-RRS cross section for Cu (points) and a non-linear fitting to an expression with the functional form of the theoretical cross section (solid line)

$$\frac{d\sigma(E_0,E_S)}{dE_S} = G(E_0,E_S)\,\frac{E_S}{\left(\Omega_K-\Omega_L-E_S\right)^2+\Gamma_K^2}$$

$$y = \frac{A}{(B-x)}$$

MC Valentinuzzi *et al.*, *X-Ray Spectrometry* **37**, 555-560 (2008).

Influence on XRF Analysis

J. Sherman, *Spectrochim. Acta* **7**, 283 (1955).
T. Shiraiwa and N. Fujino, *Jpn. J. Appl. Phys.* **5**, 886 (1966).

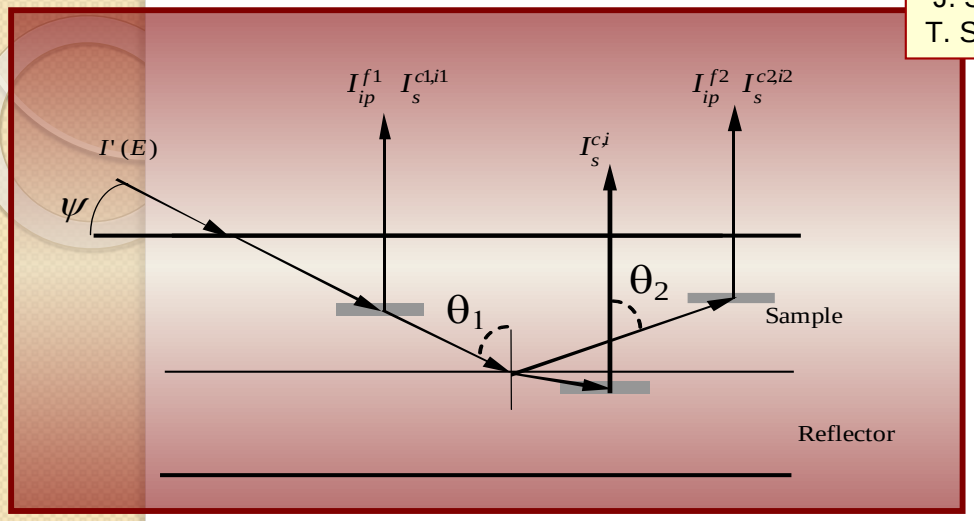

$$Q_k^f(E) = C_k\ \omega_k\ f_k\ J_k\ \tau_k\ (E)$$

$$Q_k^{c,i}(E) = \sum_{k=1}^{N} C_k\ \sigma_k^{c,i}(E)$$

$$Q_i^r(E,E') = \int_0^{E-\Omega_{\mathrm{Li}}+\mathrm{Ef}} \frac{H^R(E)\ R_z\ E'}{(\Omega_{Ki}-E)[\,(\Omega_{\mathrm{Ki}}-\Omega_{Li}-E')^2 - Ef^2]}\ dE'$$

$$^1I_i^x = \int_0^{E_{\max}} \int_0^{E_{\max}} \frac{\Delta}{4\pi} \frac{I_0(\tilde{E})Q_i^x(\tilde{E},E')}{\mu_s(\tilde{E})-\mu_s(E')G}\, d\tilde{E}\, \frac{e^{-\frac{(E-E')^2}{2\delta^2}}}{\sqrt{2\pi}\delta}\, dE'$$

$$^2I_i^{x,y} = \int_0^{E_{\max}} \sum_{k=1}^{N} \int_0^{E_{\max}} \frac{\Delta}{8\pi} \frac{I_0(\tilde{E})Q_k^x(\tilde{E},E'')Q_i^y(E'',E')}{\mu_s(\tilde{E})-\mu_s(E')G} \left\{ \frac{\cos\theta_1}{\mu_s(E'')} \ln\left[1+\frac{\mu_s(\tilde{E})}{\mu_s(E'')\cos\theta_1}\right] + \frac{\cos\theta_2}{\mu_s(E')} \ln\left[1+\frac{\mu_s(E')}{\mu_s(E'')\cos\theta_2}\right] \right\} d\tilde{E}\, \frac{e^{-\frac{(E-E')^2}{2\delta^2}}}{\sqrt{2\pi}\delta}\, dE'$$

Influence on XRF Analysis

Analysis of impurities in silicon wafers by TXRF. The combination of VPD method and SR allows DL of 10^7 at/cm^2. For Al impurities, Raman peak has to be considered!

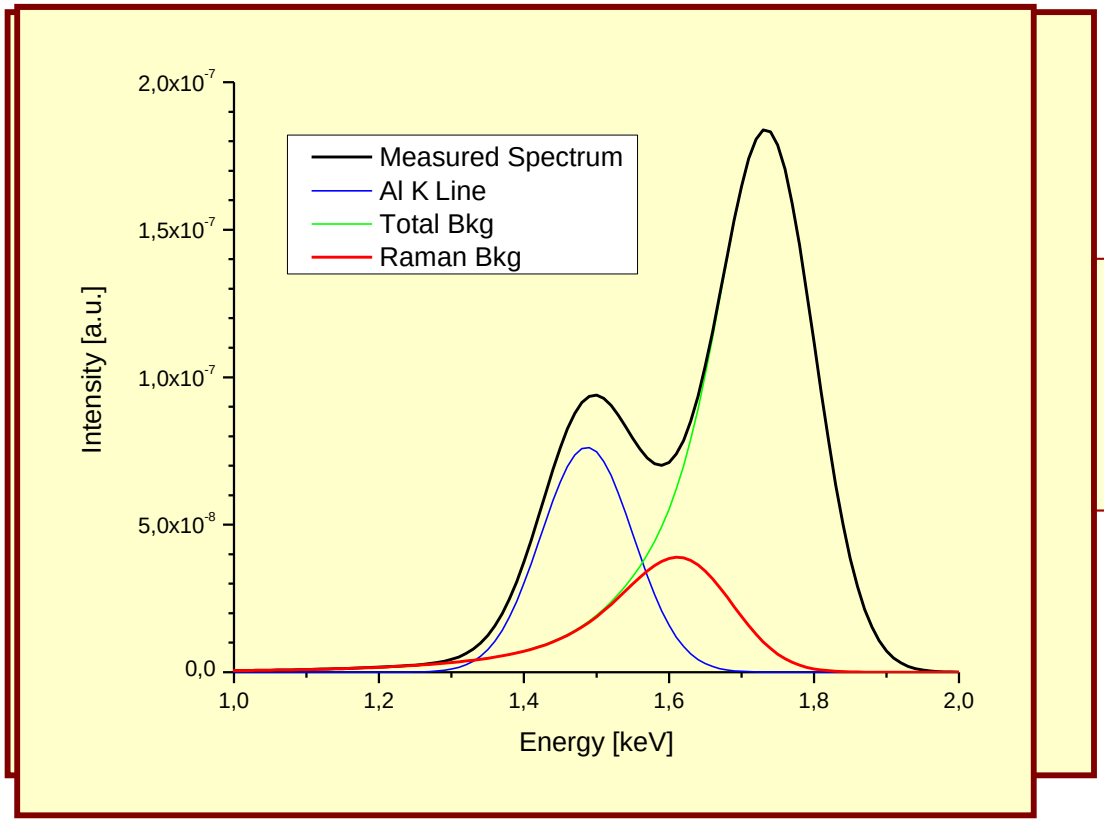

Calculated spectrum of Si (0.9995) with Al impurities (0.0005) irradiated with monochromatic photons of 1739 eV

Influence on XRF Analysis

Binary samples with proximate atomic numbers.
The Raman background competes with secondary fluorescence

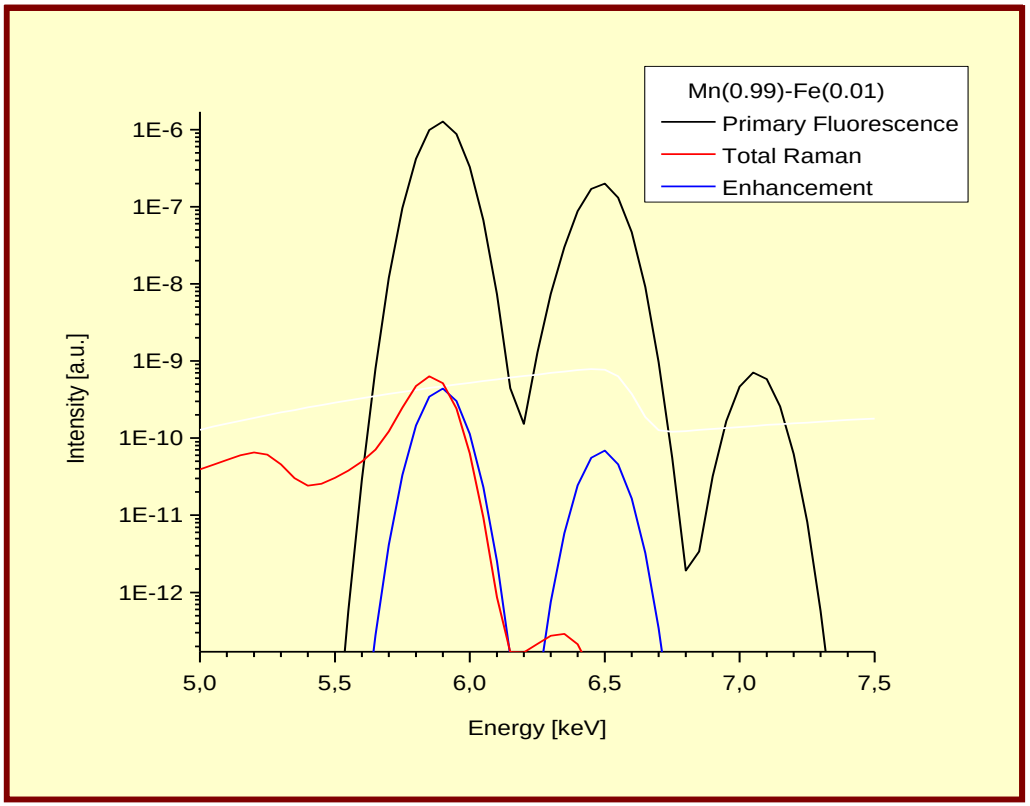

Mn Fe

Mo X-ray tube @45 kV.
Detector of 150 eV.

Influence on XRF Analysis

Binary samples with proximate atomic numbers.
The Raman background competes with secondary fluorescence

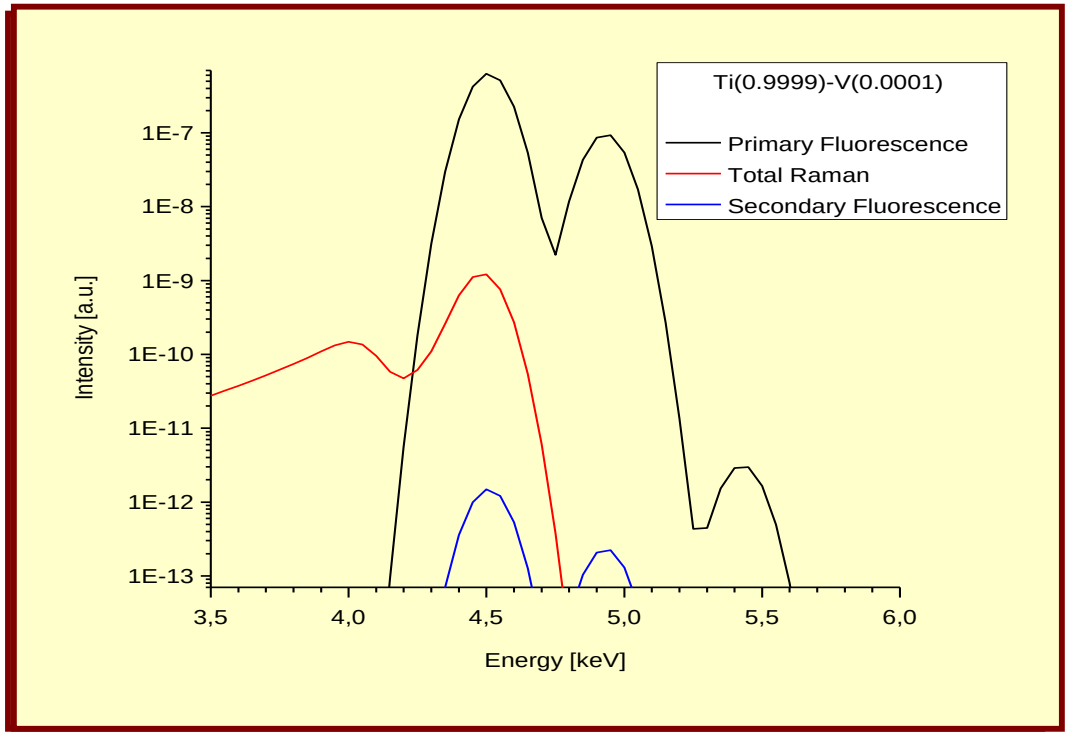

Ti V

Mo X-ray tube @45 kV.
Detector of 150 eV.

Local Environment

Possibility of studying the atomic environment

...but

There is no theory behind it yet

... meanwhile

Qualitative analysis can be carried out

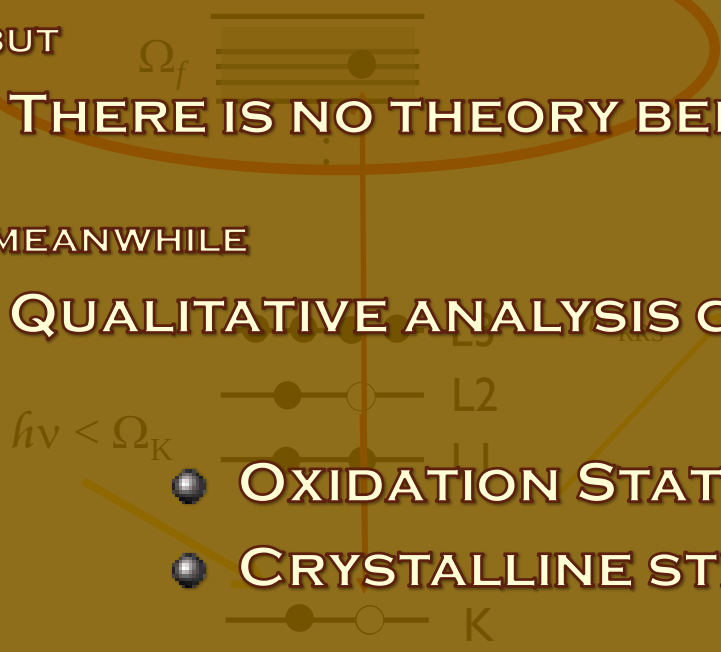

- Oxidation State
- Crystalline structure

Oxidation State Observation

Measurements performed at the LNLS (Campinas, Brazil)

- D09B- XRF Beamline
- Channel-Cut Monochromator
- Ultra-LEGe Detector
- Orthogonal Geometry (45º + 45º)
- Cu, CuO, CuO_2, Fe, Fe_2O_3, Fe_3O_4, Mn, Mn_2O_2

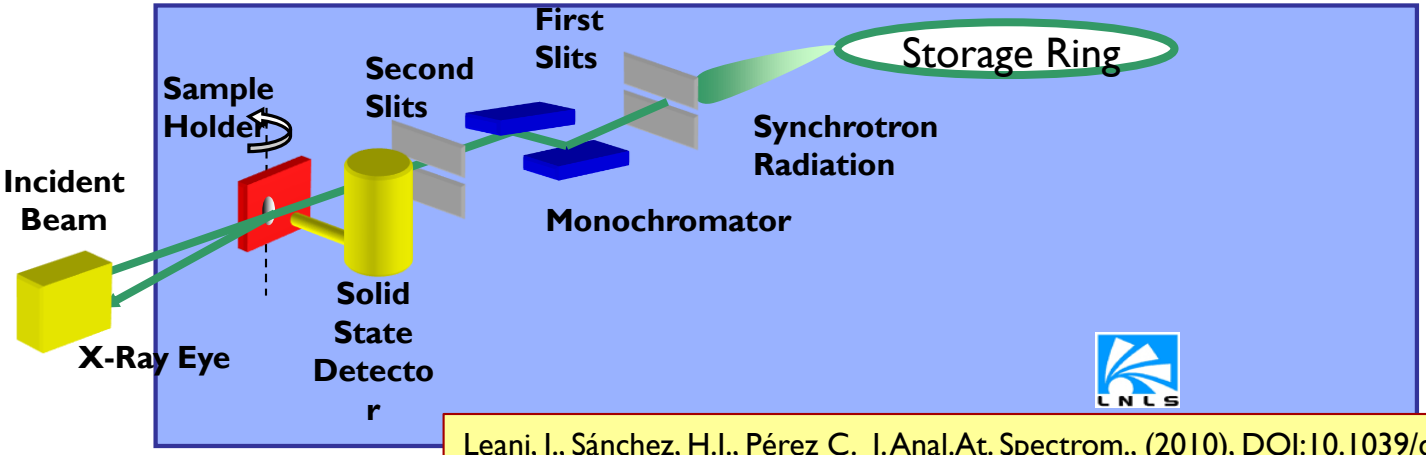

Leani, J., Sánchez, H.J., Pérez C. J.Anal.At. Spectrom., (2010), DOI:10.1039/c0ja00046a

Oxidation State Observation

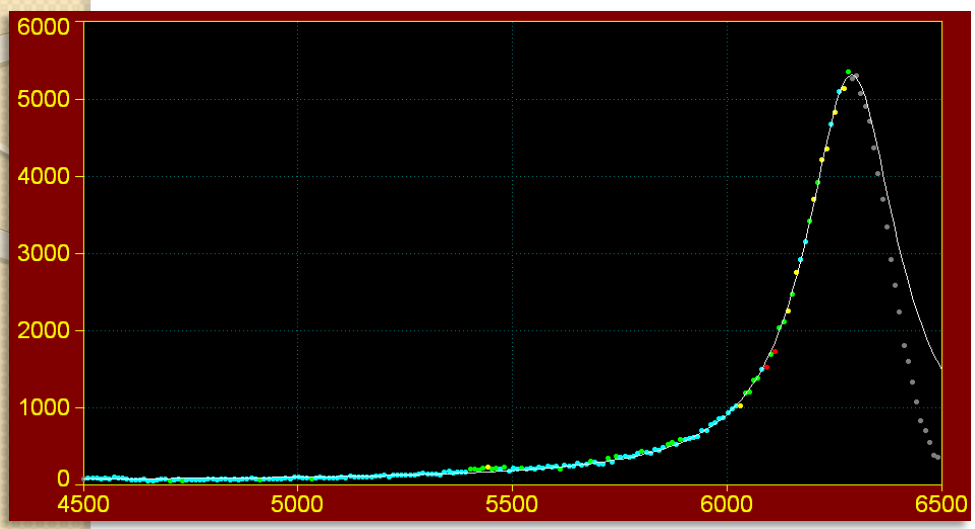

KL-RRS spectrum obtained for a Fe sample with incident energy of 7022 eV.
Solid lines represent data fitting.

DATA ANALYSIS

- Peak fitting using theoretical equations
- Residuals separation
- FFT denoising with "gaussian" instrumental function

Oxidation State Observation

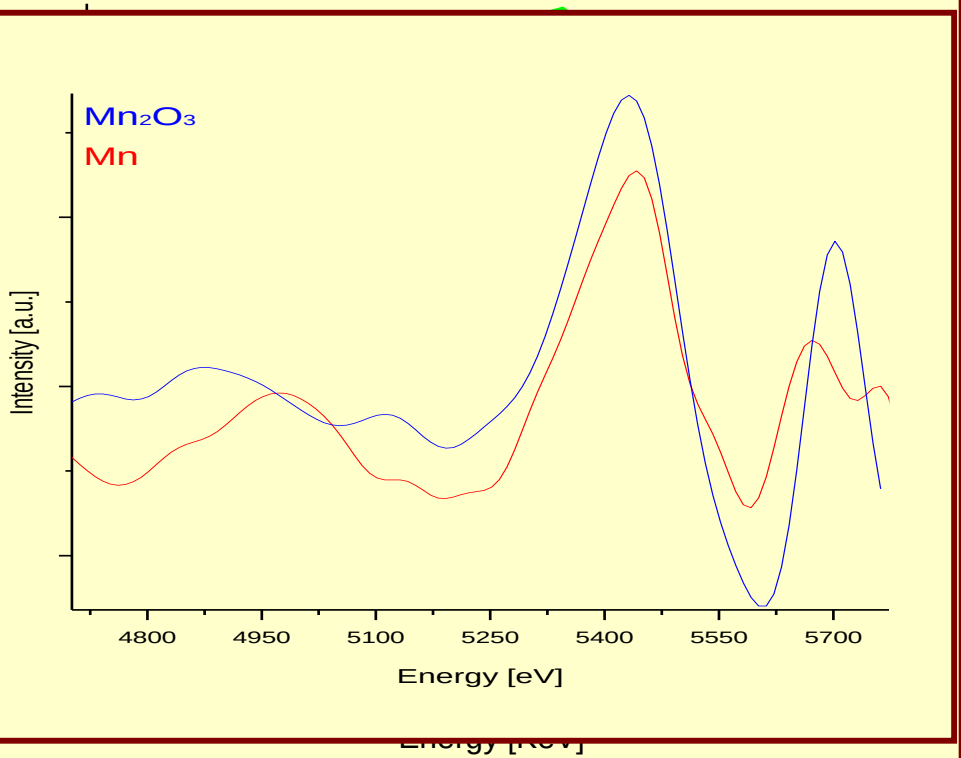

Mn, and Mn_2O_3 residuals of the experimental Raman spectra. Incident energy of 6450 eV.

RRS and EXAFS

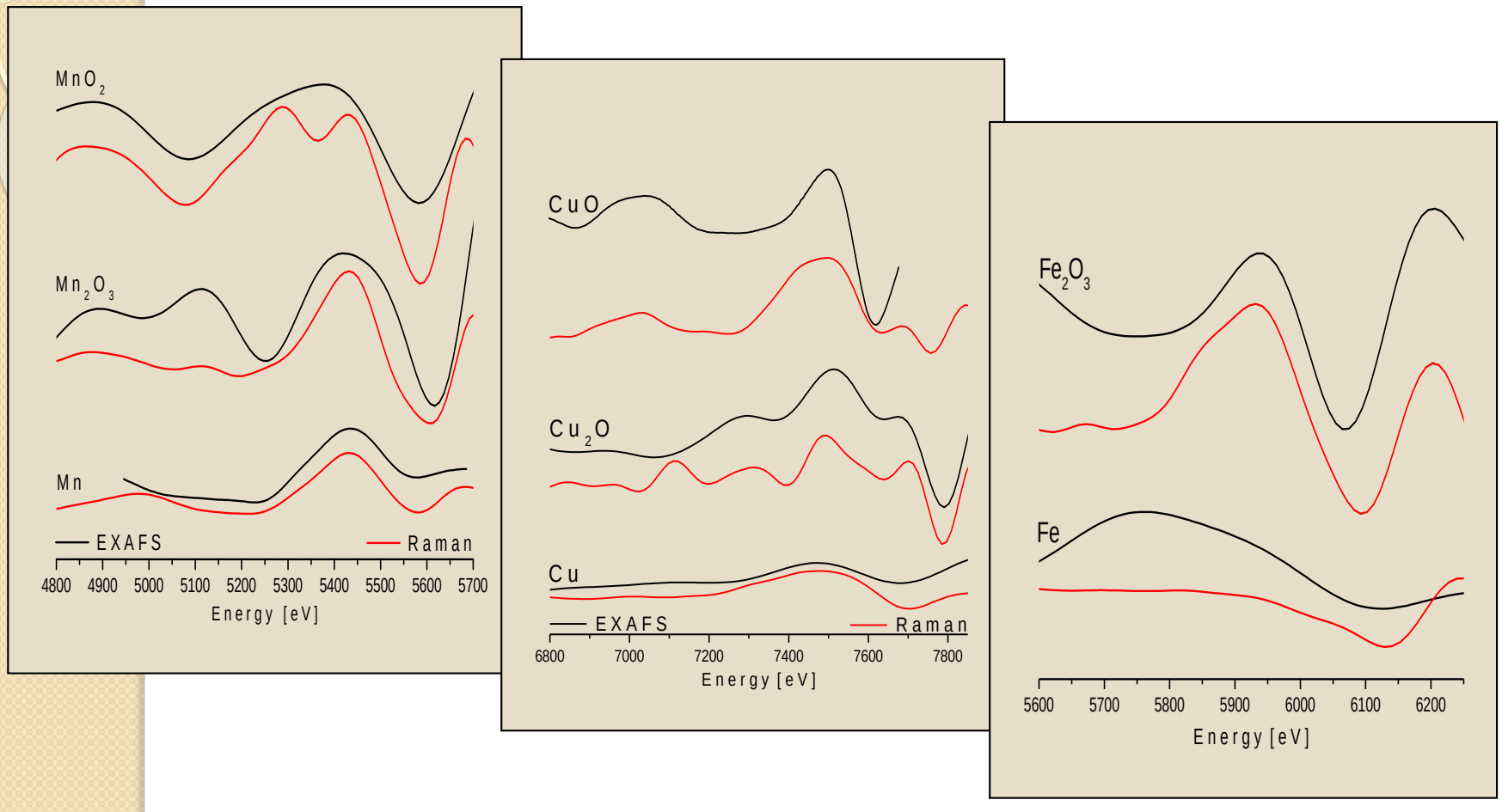

Figures show the comparison between RRS residuals and EXAFS patterns, after data processing, for: **(a)** Mn compounds, **(b)** Fe samples, and **(c)** Cu species.

"Non Conventional" RRS

Most of the techniques and methods employed in XRF can be combined with RRS analysis

(i.e. μ-RRS)

GI-RRS

Spatially Resolved RRS Spectroscopy

Confocal μ-XRF

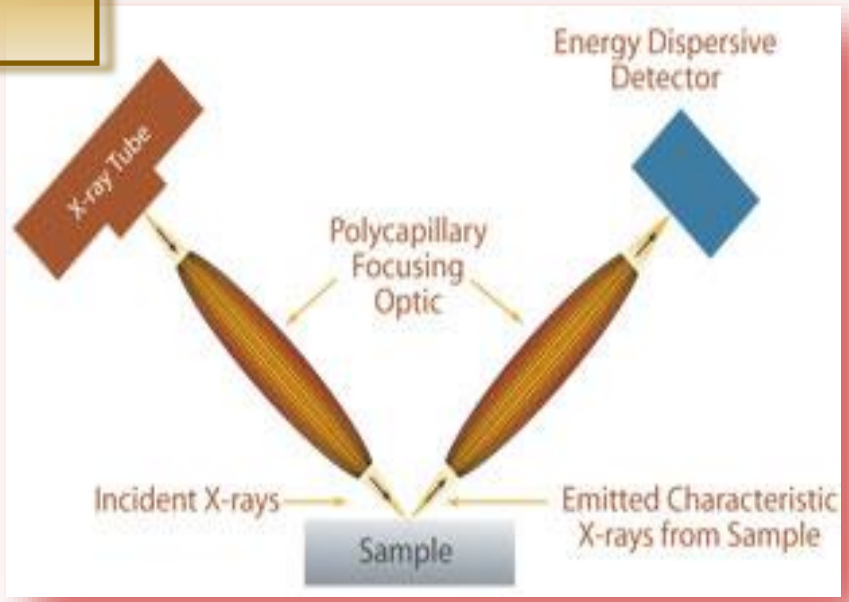

Spatially Resolved RRS Spectroscopy

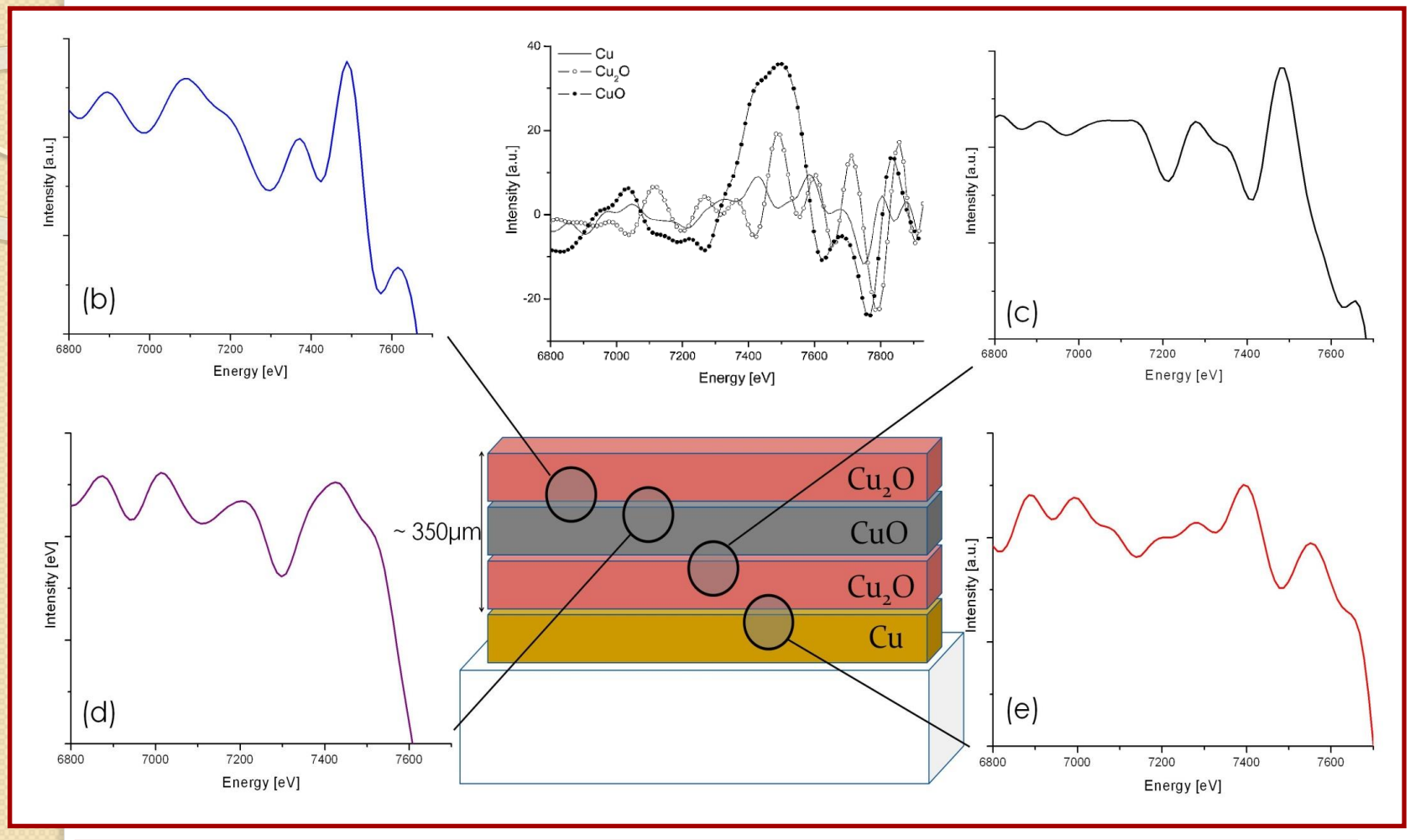

RRS residuals of Cu-oxide standards (a) and a stratified sample (b)-(e). Confocal volumen ≅ 90µm.

Spatially Resolved RRS Spectroscopy

μ-RRS Analysis of Dental Tissues

- Samples: polished cross-sections of teeth.
- Element Analysed: Calcium
- Incident Energy: 4005 eV.
- Spatial Resolution: 150 × 150 μm

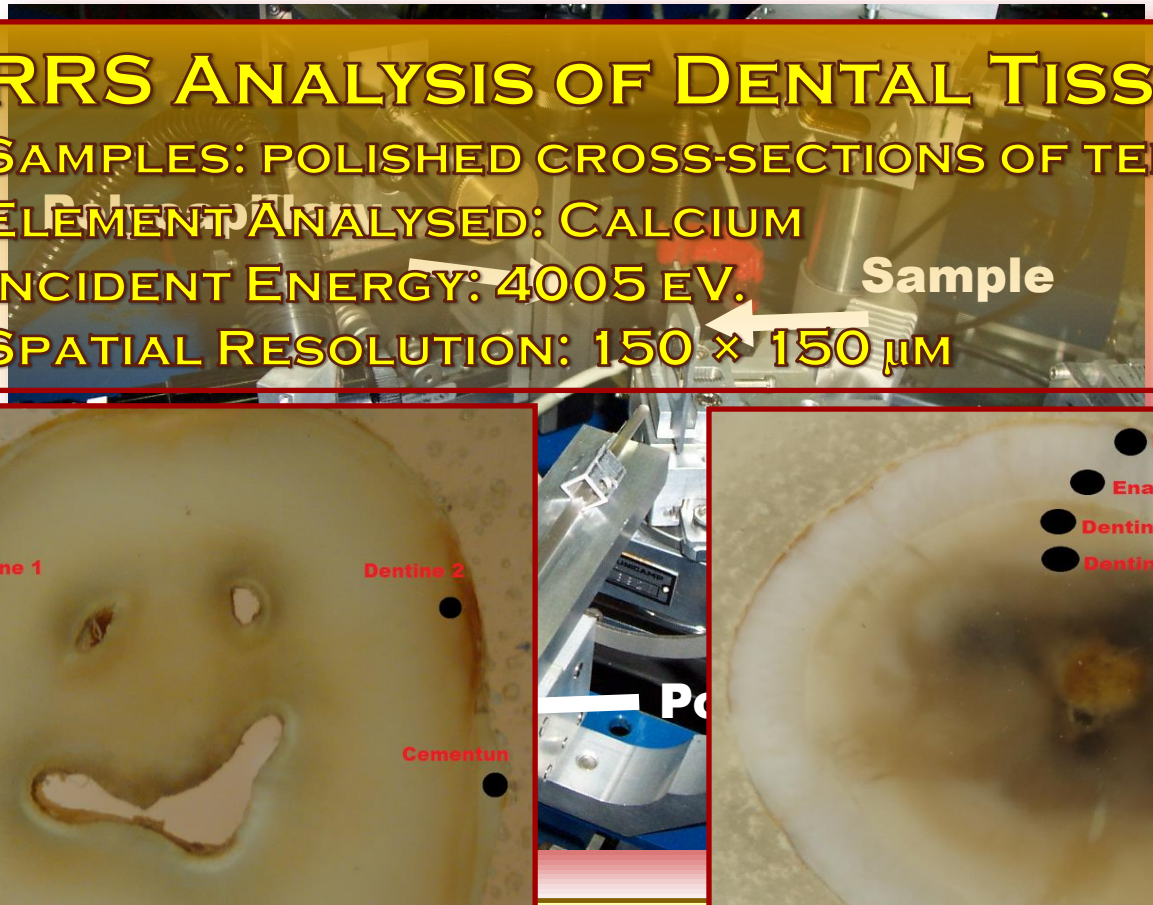

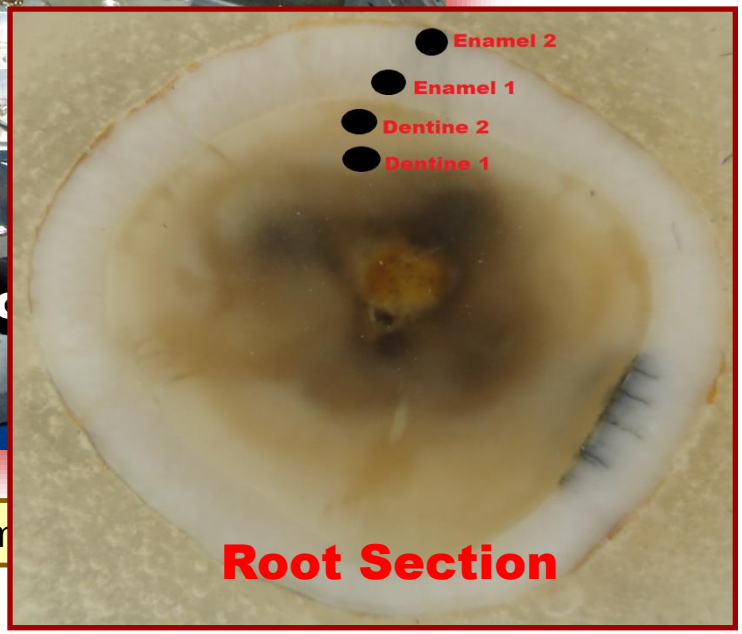

Spatially Resolved RRS Spectroscopy

Crown Section

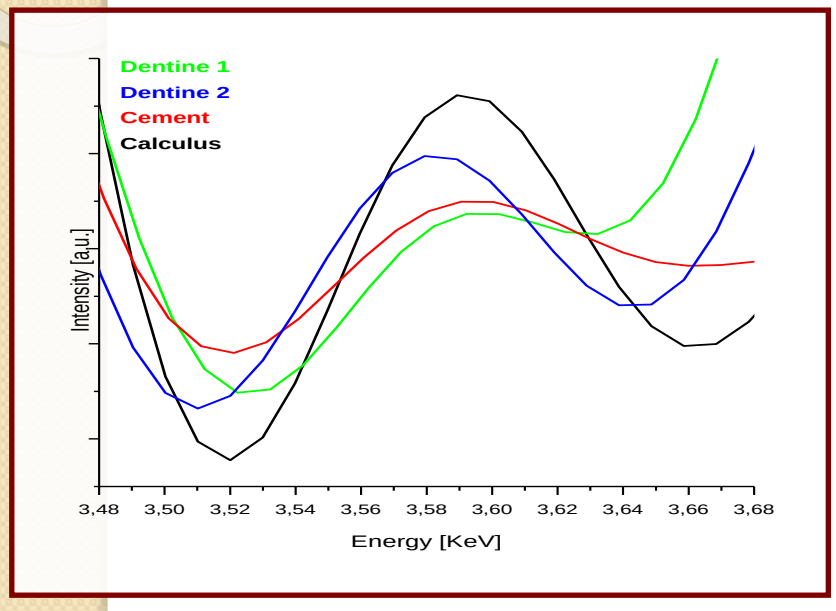

Root Section

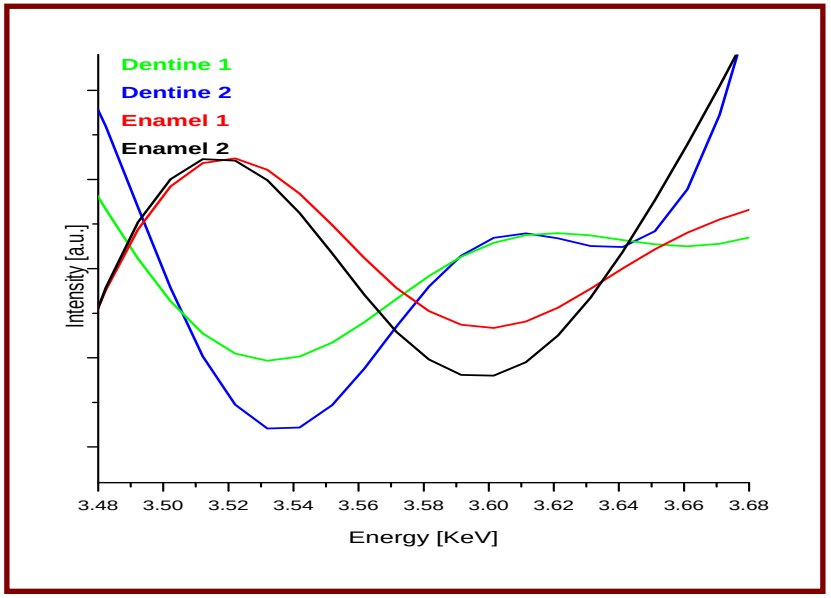

RRS in Grazing Incidence Conditions

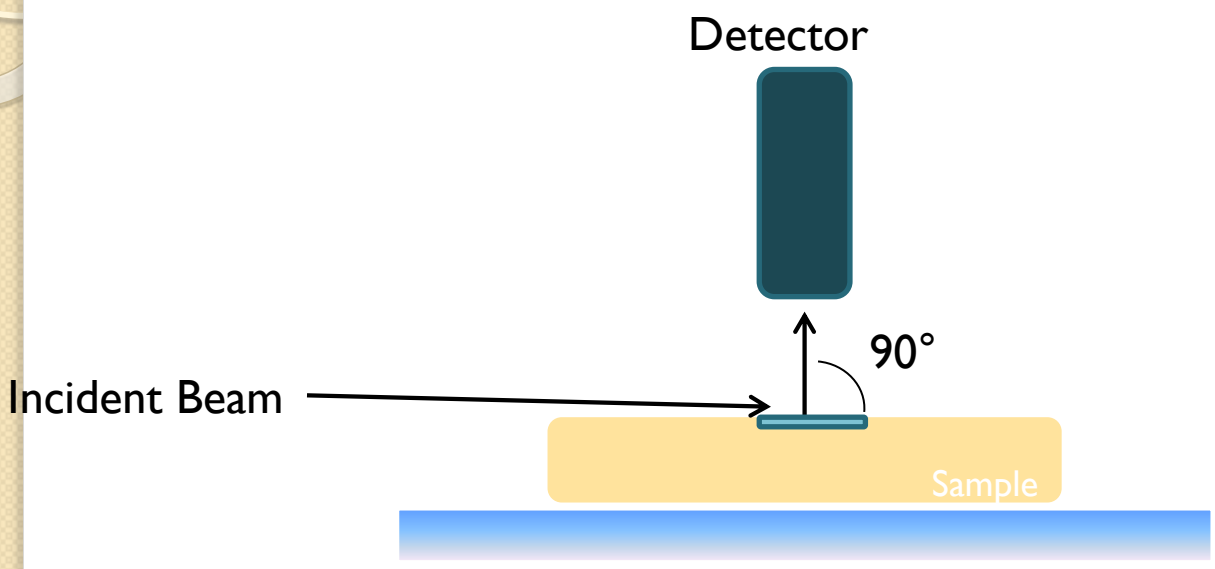

Arsenic Speciation

- Several techniques for the analysis of this element have been used and established, most of them offering a high sensitivity and very low detection limits.
- In general, the determination of species at low ranges demands chemical preconcentration and separation procedures, since most of the available instruments present a lack of the required sensitivity for direct determination and selectivity.
- The analytical methods frequently used for separation and preconcentration are solvent extraction, precipitation and coprecipitation, Ion Exchange Chromatography, Gas Chromatography (GC) and High Performance Liquid Chromatography (HPLC) .

Arsenic Speciation

Measurements performed at the LNLS
(Campinas, Brazil)

- D09B-XRF Beamline
- Channel-Cut Monochromator
- Incident Energy = 11816 eV
- Measuring Time = 3600 s.
- Atmosphere: Air
- Total Reflection Geometry
- Samples deposited on silicon wafers
- Two minerals forms : As(III) and As(IV) and Two biological forms: MMA(V) DMA(V)

Arsenic Speciation

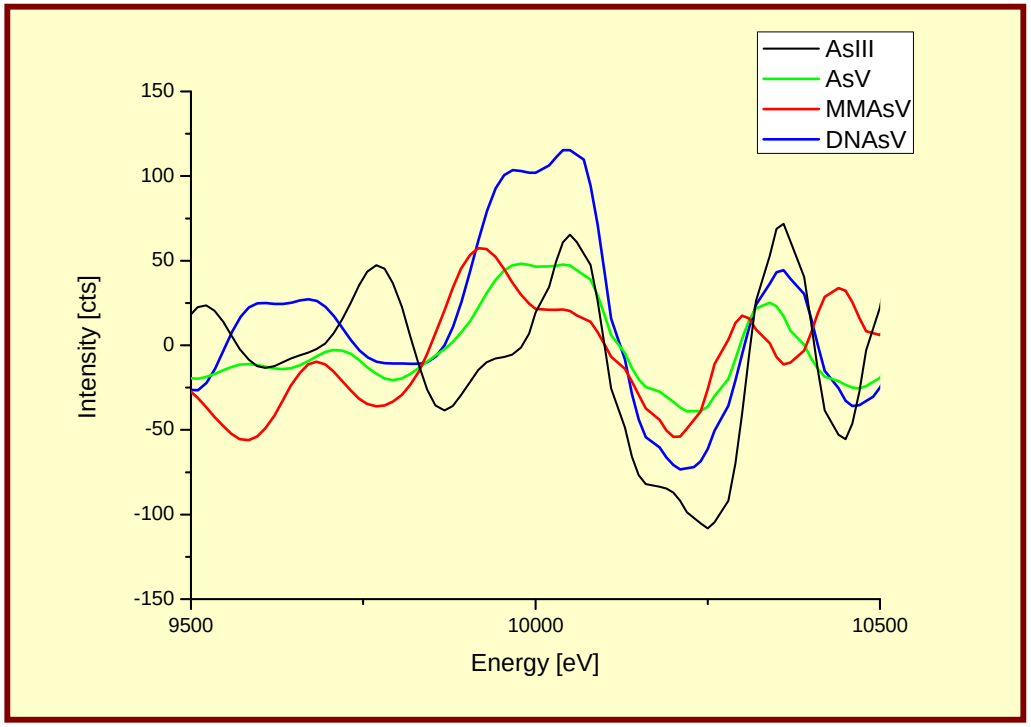

RRS residuals of the different arsenic species.

RRS in Grazing Incidence Conditions

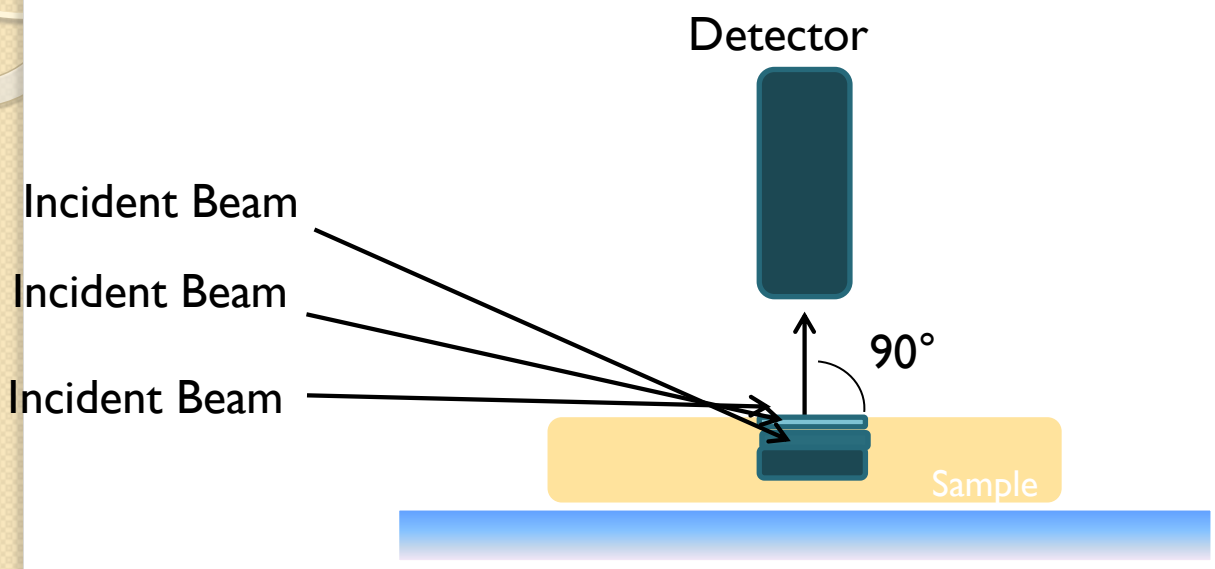

RRS in Grazing Conditions

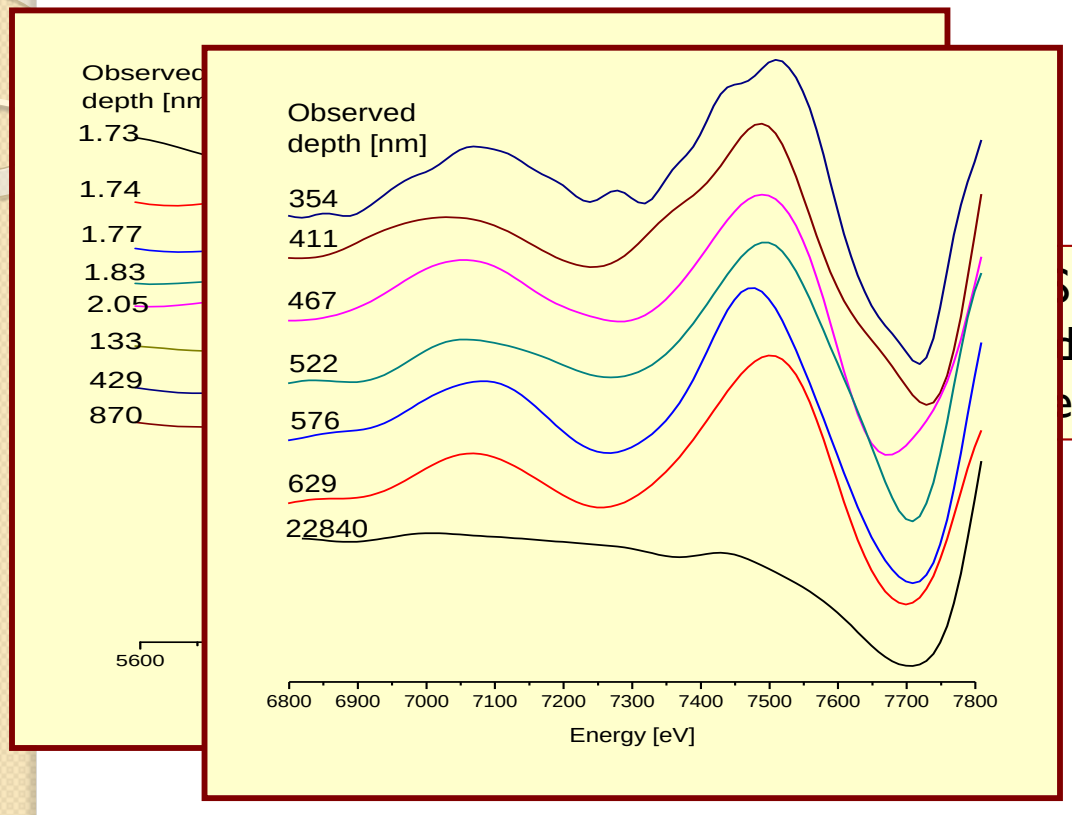

RRS residuals of an oxidized sheet of copper at different depths

RRS in Grazing Conditions

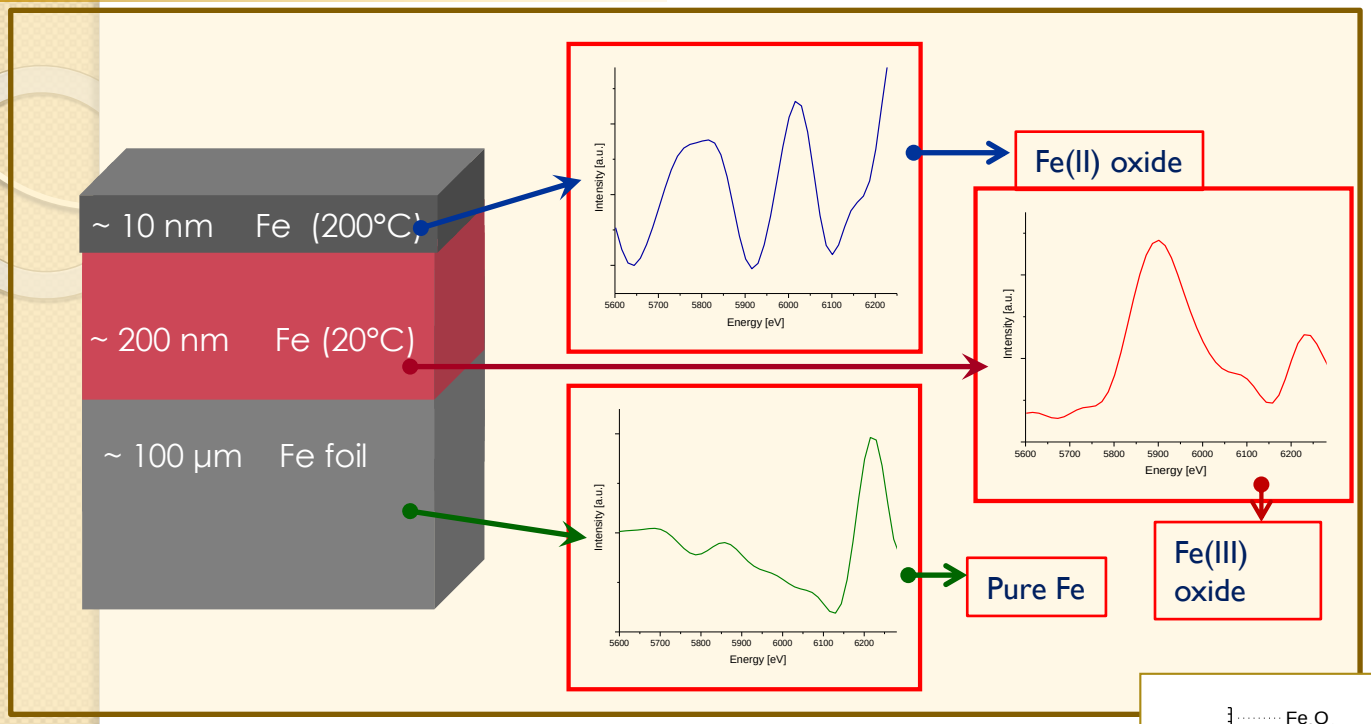

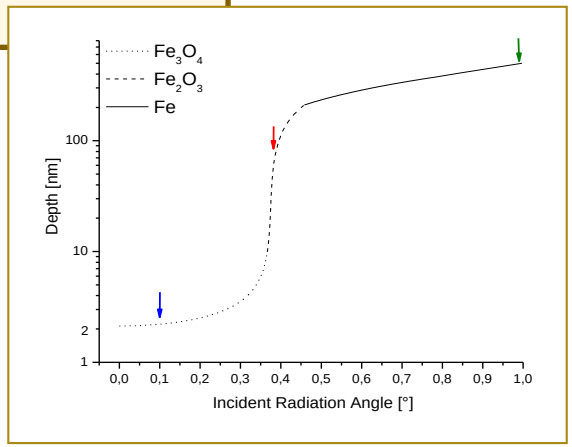

Principal Component Analysis

Preparing for data treatment

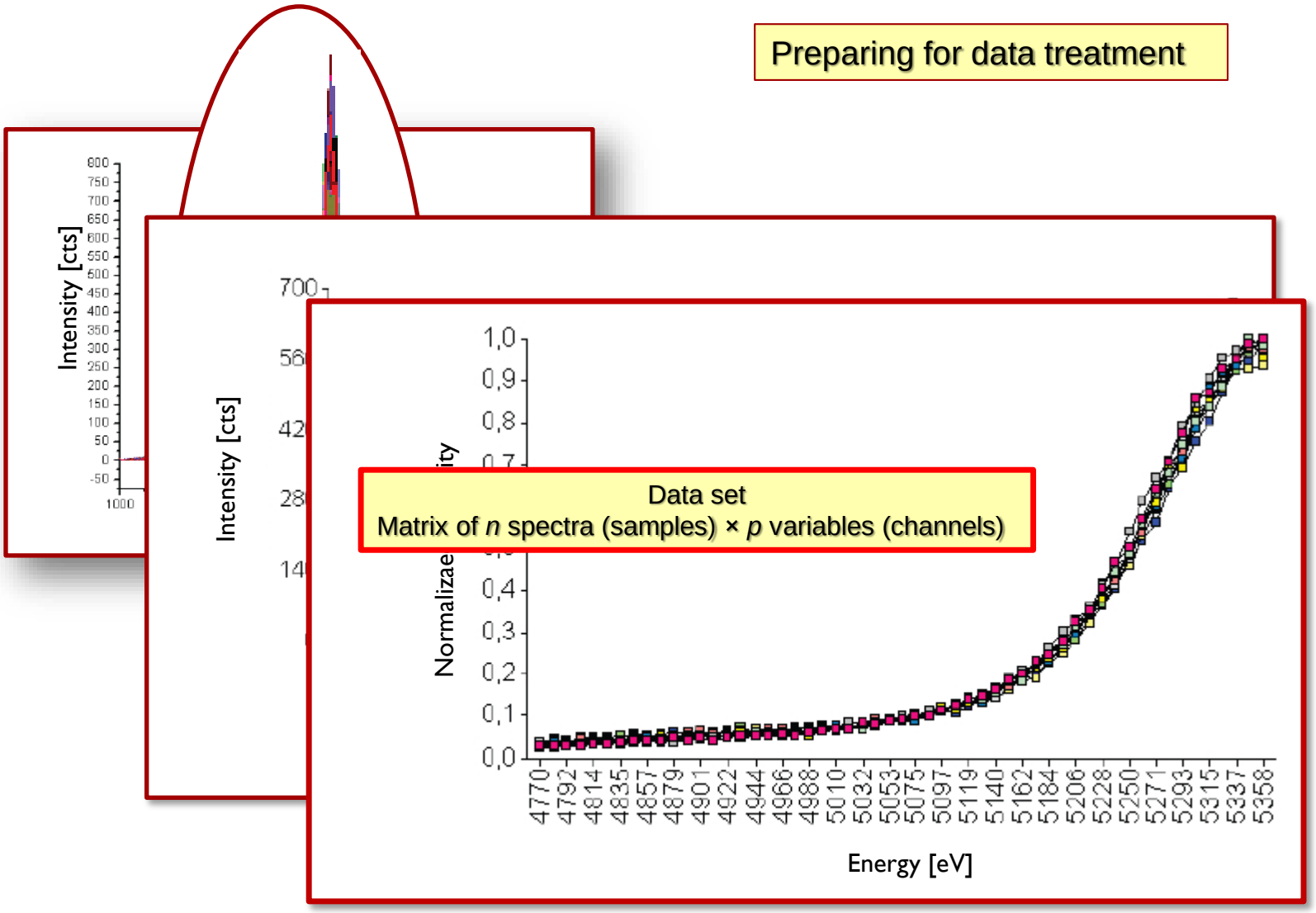

Principal Component Analysis

Water contaminated with different species of arsenic deposited on a silicon wafer.

An PCA was performed over the selected energies correlation matrix of the processed spectra, and spectra were represented in the PC1-PC2 plane.

RBS residual spectra of the different arsenic species

PCA results of the different samples (PC1 vs PC2).

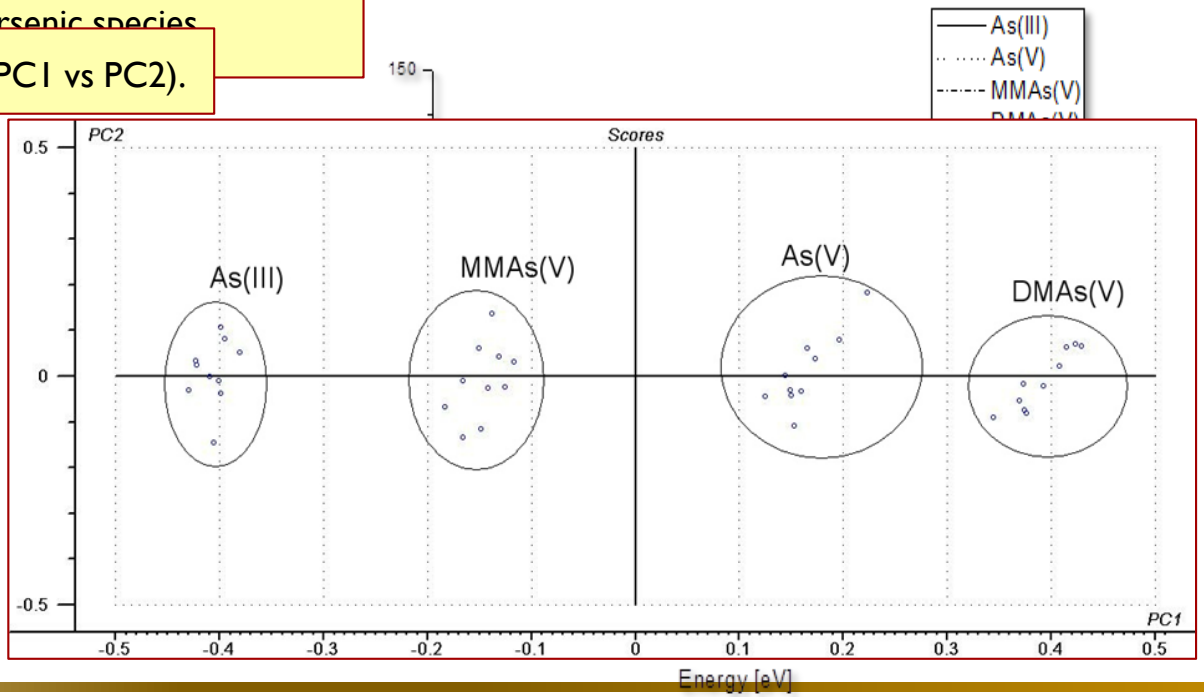

Principal Component Analysis

Surface nanolayers of Cu and Cr on a silicon wafer.

A Ward cluster analysis, with Euclidean distance, was performed on the data of the processed spectra corresponding to Cr and Cu "in situ" oxidation in order to identify different groups in the complete set of spectra. An PCA was performed over the selected energies correlation matrix of the processed spectra, and spectra were represented in the PC1-PC2 plane.

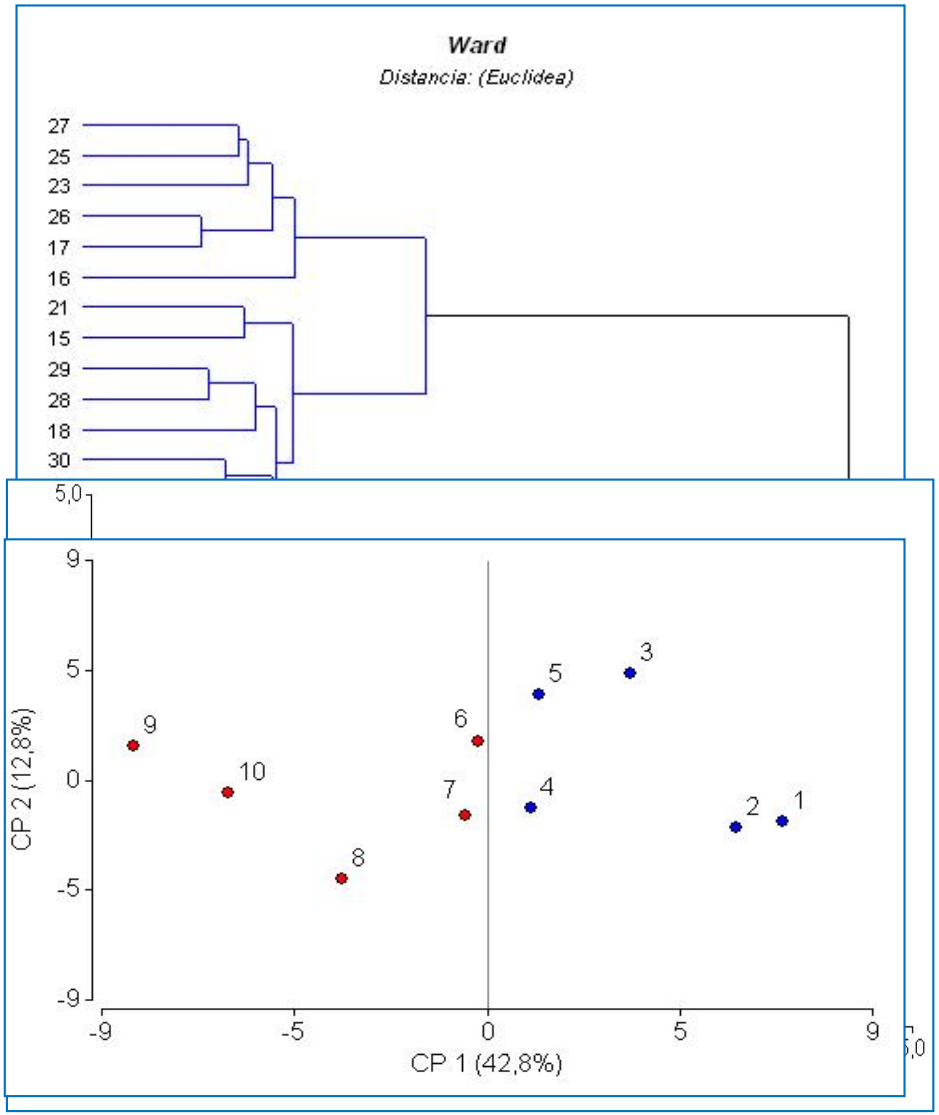

PC1-PC2 plane obtained from the PCA applied to the Cr Multilayer oxidized sample. This plane comprises a 55,6% of the data set's total variance. Blue spectra belong to the first layer of Cr_2O_3 while red spectra belong to second layer (CrO).

Dendogram obtained from the Cluster Analysis performed on the 30 spectra of the Cu "in situ" oxidized sample.

Final Comments

- Resonant Raman Scattering is a new and promising spectroscopic technique.
- The experimental methodology is very simple.
- The same non-conventional alternatives for XRF analysis can be used, in particular grazing geometries.
- It allows identifying species, oxidation states and structures.
- A theoretical models is clearly needed in order to achieve a better understanding of the experimental data.
- Multivariate Methods and PCA allows to simplify the data analysis and produce more reliable results.
- This is a promising technique, a significant work on interpretation of results is necessary.

Thank you for your attention